Nickel Thioether Chemistry: Syntheses and Crystal Structures of $[Ni_2L_2(\mu\text{-}Cl)_2][BF_4]_2$ (L = 1,4,7,10-tetrathiacyclododecane, 1,4,8,11-tetrathiacyclotetradecane or 1,5,9,13-tetrathiacyclohexadecane) †

Alexander J. Blake, Malcolm A. Halcrow and Martin Schröder *
Department of Chemistry, The University of Edinburgh, West Mains Road, Edinburgh EH9 3JJ, UK

Reaction of $NiCl_2$ with 1 molar equivalent of the macrocycles (L) 1,4,7,10-tetrathiacyclododecane ([12]aneS_4), 1,4,8,11-tetrathiacyclotetradecane ([14]aneS_4) or 1,5,9,13-tetrathiacyclohexadecane ([16]aneS_4) and $NaBF_4$ in $MeNO_2$ for 30 min afforded green or blue solutions, from which the complexes $[Ni_2L_2Cl_2][BF_4]_2$ can be isolated. The complex $[Ni_2([12]aneS_4)_2Cl_2][BF_4]_2\cdot 2MeNO_2$ crystallises in the monoclinic space group *C*2/*m* with *a* = 11.0651(20), *b* = 13.4977(24), *c* = 12.7222(21) Å, β = 104.824(21)° and *Z* = 2. The complex $[Ni_2([14]aneS_4)_2Cl_2][BF_4]_2\cdot 6MeNO_2$ crystallises in the triclinic space group $P\bar{1}$ with *a* = 10.6341(18), *b* = 11.6481(22), *c* = 12.2457(25) Å, α = 88.547(7), β = 67.288(12), γ = 68.647(6)° and *Z* = 1. The complex $[Ni_2([16]aneS_4)_2Cl_2][BF_4]_2\cdot 2MeNO_2$ crystallises in the monoclinic space group *Cc* with *a* = 16.024(4), *b* = 13.6862(17), *c* = 19.7329(24) Å, β = 92.042(19)° and *Z* = 4. Single-crystal structure determinations on each of these products showed the presence of dichloro-bridged dimeric cations exhibiting edge-sharing bioctahedral structures, with the macrocyclic ligands co-ordinated in a *cis* fashion about the Ni. The Ni–S bond lengths and internal crystallographic symmetry vary significantly between the structures, the shortest distances being observed for $[Ni_2([14]aneS_4)_2Cl_2]^{2+}$ [Ni–S 2.3694(22), 2.3765(21), 2.3756(21), 2.3798(21) Å, Ni–Cl 2.4416(20), 2.4252(20) Å]; for $[Ni_2([12]aneS_4)_2Cl_2]^{2+}$, Ni–S 2.412(3), 2.4144(25), 2.373(3), Ni–Cl 2.411(3), 2.382(3) Å and for $[Ni_2([16]aneS_4)_2Cl_2]^{2+}$, Ni–S 2.4098(22)–2.4421(22), Ni–Cl 2.3860(21)–2.4205(20) Å. These variations are related to the differing hole sizes of the three tetrathia macrocyles. The Ni···Ni distances are similar in all three structures, 3.5534(12)–3.5692(12) Å. The complexes $[Ni_2L_2Cl_2][BF_4]_2$ exhibit only irreversible electrochemical oxidation and reduction processes according to cyclic voltammetry in MeCN–0.1 mol dm^{-3} $NBu^n{}_4PF_6$ at 293 K. Reaction of $NiCl_2$ with 1,4,7-trithiacyclononane ([9]aneS_3) and $NaBF_4$ affords the triply bridged dimeric complex $[Ni_2([9]aneS_3)_2Cl_3]BF_4$.

The co-ordination chemistry of nickel with sulfur-donor ligands is the subject of intense interest. Redox active nickel centres in hydrogenase and CO-oxido-reductase enzymes are known to be bound in sulfur-rich environments,[1] and several classes of model compounds for these biological systems containing thiolate or thioether ligands have been investigated.[2,3] As part of our studies on the co-ordination chemistry of polythia macrocyclic ligands[4] we have investigated the complexation chemistry of tri-, tetra- and penta-thia crowns with nickel(II).[5-7] We report here the syntheses and single crystal structures of the chloro-bridged bioctahedral dimeric species $[Ni_2L_2Cl_2]^{2+}$ {L = 1,4,7,10-tetrathiacyclododecane ([12]aneS_4), 1,4,8,11-tetrathiacyclotetradecane ([14]aneS_4) and 1,5,9,13-tetrathiacyclohexadecane ([16]aneS_4)}.

The first nickel(II) crown thioether complexes were reported by Rosen and Busch,[8] who prepared the square-planar species $[Ni([14]aneS_4)]^{2+}$ and the octahedral complexes $[Ni([14]aneS_4)X_2]$ (X = Cl, Br or I). A single-crystal structure determination of $[Ni([14]aneS_4)][BF_4]_2$ confirmed the proposed square-planar geometry at Ni^{II}.[9] The reaction of $[Ni(OH_2)_6]^{2+}$ with L = [12]aneS_4 or 1,4,7,11-tetrathiacyclotridecane ([13]aneS_4) was also reported to give the dimeric species $[Ni_2L_3]^{4+}$ containing both endo- and exo-dentate co-ordinated ligands, although these products were not fully

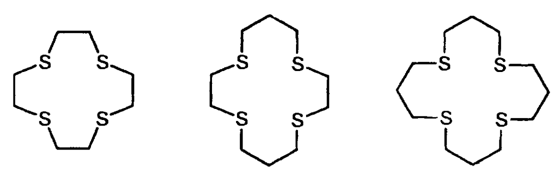

[12]aneS_4 [14]aneS_4 [16]aneS_4

characterised.[10] The syntheses and single-crystal structures of several homoleptic octahedral NiS_6 complexes containing tri- or hexa-thia macrocycles have also been reported.[6,11,12] Recently, we have shown that the complexation of Ni^{II} by L = [12]aneS_4 or [16]aneS_4 in the absence of co-ordinating anions leads to the octahedral complexes $[NiL(solv)_2]^{2+}$ (solv = H_2O or MeCN).[7] We were therefore interested in re-examining the nickel(II) chemistry of the tetrathia crowns in the presence of anions such as chloride.

Results and Discussion

The reaction of anhydrous $NiCl_2$ with 1 molar equivalent of [12]aneS_4 or [16]aneS_4 in $MeNO_2$ at 293 K for 30 min gave a pale green precipitate. Addition of $NaBF_4$ and mild heating of the reaction mixture led to dissolution of the precipitate, affording a green solution and a white precipitate of NaCl. Removal of NaCl by filtration, reduction of the solution and addition of Et_2O yielded green microcrystalline solids in

† *Supplementary data available:* see Instructions for Authors, *J. Chem. Soc., Dalton Trans.*, 1994, Issue 1, pp. xxiii–xxviii.

65–70% yield. An analogous complexation reaction using [14]aneS_4 afforded a blue microcrystalline solid product, in 62% yield. Infrared spectroscopy and microanalytical data were consistent with the formulations [Ni(L)Cl]BF_4 (L = [12]aneS_4, [14]aneS_4 or [16]aneS_4) for these products. However, FAB mass spectrometry showed, in addition to peaks from monomeric fragments, strong peaks corresponding to binuclear molecular ions. For example, for L = [12]aneS_4, peaks were observed at *m/z* = 753, 666, 333 and 298 assigned to [$^{58}Ni_2$([12]aneS_4)$_2$$^{35}Cl_2$($^{11}BF_4$)]$^+$, [$^{58}Ni_2$([12]ane$S_4$)$_2$-$^{35}Cl_2$]$^+$, [^{58}Ni([12]ane$S_4$)^{35}Cl]$^+$ and [^{58}Ni([12]aneS_4)]$^+$ respectively. The three products were therefore assigned as dimeric species [Ni_2L_2(μ-Cl)$_2$][BF_4]$_2$ with two chloride bridging ligands. The electronic spectra of the complexes in MeCN solution each exhibited three weak d–d bands. For example for L = [12]aneS_4, λ_{max} = 980 (ε_{max} = 25.6), 608 (30.7) and 384 nm (93.2 dm^3 mol^{-1} cm^{-1}). This is typical of octahedrally co-ordinated nickel(II) centres,[13] and supports the above formulation.

Halide- or pseudo-halide-bridged dimeric structures are well known both for nickel(II)[13] and for other metal centres.[14] For Ni^{II}, examples containing octahedral and trigonal-bipyramidal centres with one, two or three bridging ligands have been structurally characterised.[15–19] Previously reported halide- or pseudo-halide-bridged nickel(II) dimers containing macrocyclic ligands include [Ni_2(Me_4[14]aneN_4)$_2$(N_3)$_2$(μ-N_3)]$^+$ (Me_4-[14]aneN_4 = 1,4,8,11-tetramethyl-1,4,8,11-tetraazacyclotetradecane),[16] [$Ni_2L^1{}_2$(μ-C_2O_4)]$^{2+}$ (L^1 = 5,5,7,12,12,14-hexamethyl-1,4,8,11-tetraazacyclotetradecane)[17] and the triply bridged complex [Ni_2(Me_3[9]aneN_3)$_2$(μ-$MeCO_2$)$_2$(μ-OH)]$^+$ (Me_3[9]aneN_3 = 1,4,7-trimethyl-1,4,7-triazacyclononane).[18] Few binuclear complexes incorporating thioether donors have been prepared and these include [Ni_2{N($CH_2CH_2SPr^i$)$_3$}$_2$(μ-Cl)$_2$]$^{2+}$ (ref. 3) and [$Ni_2L^2{}_2$(μ-Cl)$_2$]$^{2+}$ [L^2 = 1,7-bis(benzimidazol-2-yl)-2,6-dithiaheptane].[20]

In order to confirm the dimeric nature of these products, and to investigate the effect of macrocyclic hole size on the metal–ligand and –metal interactions in such compounds, single-crystal X-ray analyses of the BF_4^- salts of each of these complex cations were undertaken. Diffusion of Et_2O vapour into $MeNO_2$ solutions of the complexes afforded crystals of X-ray quality. In all three cases rapid solvent loss from these crystals was observed on exposure to air. The single-crystal structure determinations confirmed the proposed doubly bridged bioctahedral structures, [Ni_2L_2(μ-Cl)$_2$]$^{2+}$ (Figs 1–3, Tables 1–6), with each Ni atom bound to a *cis*-S_4Cl_2 donor set.

The structure of [Ni_2([12]aneS_4)$_2Cl_2$][BF_4]$_2$·2$MeNO_2$ shows the complex cation to possess crystallographically imposed 2/*m* symmetry, with the Ni_2Cl_2 bridge and equatorial S donors S(1) and S(7) lying on a crystallographic mirror plane and with an inversion centre at the midpoint of the Ni···Ni vector. The complex exhibits a tetragonal shortening along the S(7)–Ni–Cl axis [Ni–S(1) 2.412(3), Ni–S(4) 2.414(3), Ni–S(7) 2.373(3), Ni–Cl 2.411(3), Ni–Cl′ 2.382(3) Å]. This contrasts with the related complex [Ni_2(en)$_4$(μ-Cl)$_2$]$^{2+}$ (en = 1,2-diaminoethane) which exhibits a tetragonal elongation along the same axis,[19] reflecting the presence of a π-acceptor S-donor *trans* to a π-donor Cl^- ligand, as opposed to a purely σ-donating diamine ligand. The Ni–S bond lengths are similar to those observed for the *trans*-octahedral complex [Ni([16]aneS_4)(OH_2)$_2$]$^{2+}$,[7] significantly longer than for nickel hexathia macrocycle complexes such as [Ni([9]aneS_3)$_2$]$^{2+}$ ([9]aneS_3 = 1,4,7-trithiacyclononane)[11] and [Ni([18]aneS_6)]$^{2+}$ ([18]aneS_6 = 1,4,7,10,13,16-hexathiacyclooctadecane),[12] but significantly shorter than in *trans*-[{$NiCl_2$(dtco)$_2$}$_n$] (dtco = 1,5-dithiacyclooctane) [Ni–S 2.478(3) and 2.497(3) Å].[21] The angles about the nickel centres in [Ni_2([12]aneS_4)$_2Cl_2$]$^{2+}$ are significantly distorted from an ideal octahedral geometry [S(1)–Ni–Cl 178.82(10), S(7)–Ni–Cl′ 170.97(10) and S(4)–Ni–S(4′) 166.14(9)°]. These general features reflect the relatively

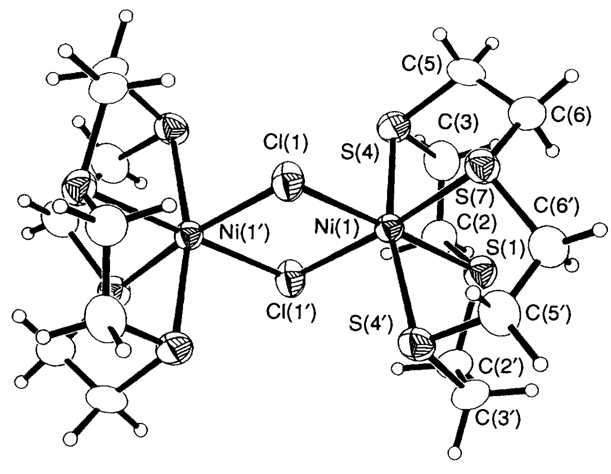

Fig. 1 View of the structure of [Ni_2([12]aneS_4)$_2Cl_2$]$^{2+}$ with the numbering scheme adopted

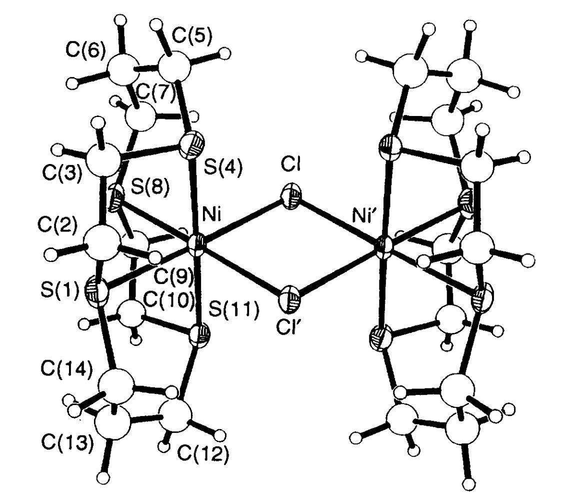

Fig. 2 View of the structure of [Ni_2([14]aneS_4)$_2Cl_2$]$^{2+}$ with the numbering scheme adopted

small cavity size of the [12]aneS_4 ligand and its mismatch with Ni^{II}. The Ni···Ni distance in [Ni_2([12]aneS_4)$_2Cl_2$]$^{2+}$ is 3.5559(17) Å and is typical for a dichloro-bridged nickel(II) dimer.[13]

The cation in [Ni_2([14]aneS_4)$_2Cl_2$][BF_4]$_2$·6$MeNO_2$ lies on a crystallographic inversion centre. The Ni–S bond lengths are *shorter* than for the corresponding dimeric complexes with [12]aneS_4 and [16]aneS_4 [Ni–S(1) 2.3694(22), Ni–S(4) 2.3765(21), Ni–S(8) 2.3756(21) and Ni–S(11) 2.3798(21) Å], a result of the improved match between the [14]aneS_4 macrocyclic cavity and the Ni^{II}.[22] The Ni–Cl and Ni···Ni distances are similar to those observed for the other dimeric cations, and the bond angles about the Ni atoms are close to 90 and 180° [Ni–Cl 2.4416(20), Ni–Cl′ 2.4252(20), Ni···Ni′ 3.5692(12) Å; S(1)–Ni–Cl 178.09(8), S(8)–Ni–Cl′ 178.07(7) and S(4)–Ni–S(11) 178.70(8)°].

In contrast, the [Ni_2([16]aneS_4)$_2Cl_2$]$^{2+}$ cation possesses no internal symmetry, with a wide spread of Ni–S and Ni–Cl bond lengths [Ni–S 2.4098(22)–2.4421(22) Å, Ni–Cl 2.3860(21)–2.4205(20) Å]. Examination of space-filling models shows (Fig. 4) that for the ligand conformation observed the imposition of a centre of symmetry between the Ni atoms would result in unfavourable steric interactions between methylene groups of the two macrocycles. Interestingly, however, a slight twisting of 1.31(7)° of the [16]aneS_4 rings relative to one another has no apparent effect on the Ni···Ni distance [Ni(1)···Ni(2) 3.5534(12) Å], which is very similar to that observed for both

Table 1 Bond lengths (Å), angles and torsion angles (°) with estimated standard deviations (e.s.d.s.) for $[Ni_2([12]aneS_4)_2Cl_2][BF_4]_2 \cdot 2MeNO_2$

Ni···Ni′	3.5559(17)	S(1)–C(2)	1.806(9)
Ni–S(1)	2.412(3)	C(2)–C(3)	1.548(12)
Ni–S(4)	2.4144(25)	C(3)–S(4)	1.823(9)
Ni–S(7)	2.373(3)	S(4)–C(5)	1.841(9)
Ni–Cl	2.411(3)	C(5)–C(6)	1.512(13)
Ni–Cl′	2.382(3)	C(6)–S(7)	1.810(9)
S(1)–Ni–S(4)	83.73(9)	Ni–S(1)–C(2)	97.0(3)
S(1)–Ni–S(7)	94.42(10)	Ni–S(4)–C(3)	103.2(3)
S(1)–Ni–Cl	178.82(10)	Ni–S(4)–C(5)	99.9(3)
S(1)–Ni–Cl′	94.61(9)	Ni–S(7)–C(6)	98.9(3)
S(4)–Ni–S(4′)	166.14(9)	C(2)–S(1)–C(2′)	107.0(4)
S(4)–Ni–S(7)	87.54(9)	S(1)–C(2)–C(3)	106.0(6)
S(4)–Ni–Cl	96.32(9)	C(2)–C(3)–S(4)	112.5(6)
S(4)–Ni–Cl′	93.44(9)	C(3)–S(4)–C(5)	101.2(4)
S(7)–Ni–Cl	86.76(9)	S(4)–C(5)–C(6)	114.5(6)
S(7)–Ni–Cl′	170.97(10)	C(5)–C(6)–S(7)	108.0(6)
Cl–Ni–Cl′	84.21(9)	C(6)–S(7)–C(6′)	106.6(4)
Ni–Cl–Ni′	95.79(9)		

C(2′)–S(1)–C(2)–C(3)	163.2(6)
S(1)–C(2)–C(3)–S(4)	−59.0(7)
C(2)–C(3)–S(4)–C(5)	125.0(6)
C(3)–S(4)–C(5)–C(6)	−75.2(7)
S(4)–C(5)–C(6)–S(7)	−60.7(7)
C(5)–C(6)–S(7)–C(6′)	157.9(6)

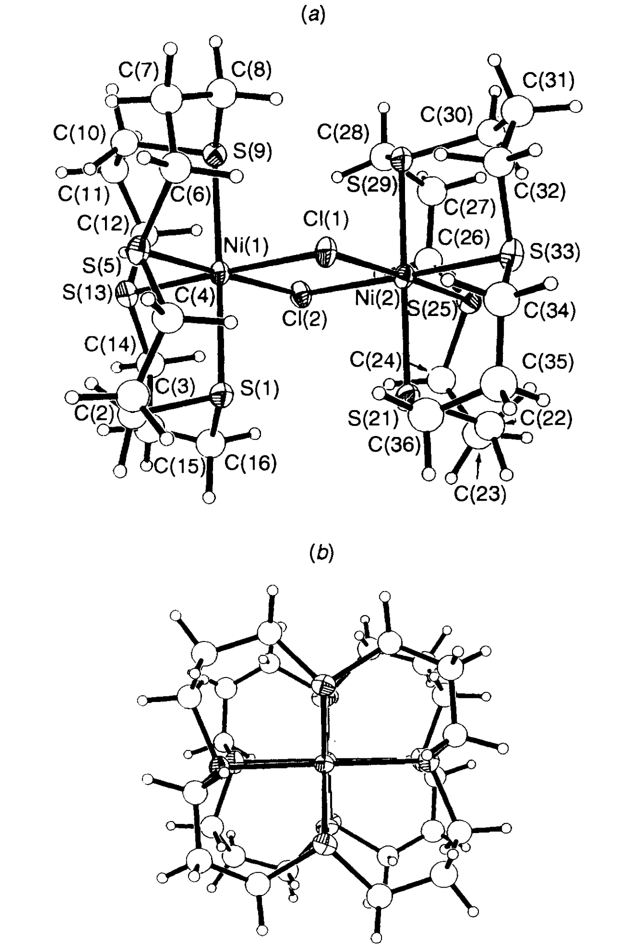

Fig. 3 Two views of the structure of $[Ni_2([16]aneS_4)_2Cl_2]^{2+}$ with the numbering scheme adopted

Table 2 Bond lengths (Å), angles and torsion angles (°) with e.s.d.s for $[Ni_2([14]aneS_4)_2Cl_2][BF_4]_2 \cdot 6MeNO_2$

Ni···Ni′	3.5692(12)	S(4)–C(5)	1.826(8)
Ni–S(1)	2.3694(22)	C(5)–C(6)	1.503(12)
Ni–S(4)	2.3765(21)	C(6)–C(7)	1.512(12)
Ni–S(8)	2.3756(21)	C(7)–S(8)	1.804(8)
Ni–S(11)	2.3798(21)	S(8)–C(9)	1.848(8)
Ni–Cl	2.4416(20)	C(9)–C(10)	1.514(11)
Ni–Cl′	2.4252(20)	C(10)–S(11)	1.829(8)
S(1)–C(2)	1.834(9)	S(11)–C(12)	1.810(9)
S(1)–C(14)	1.815(9)	C(12)–C(13)	1.507(13)
C(2)–C(3)	1.547(12)	C(13)–C(14)	1.518(12)
C(3)–S(4)	1.822(8)		
Cl–Ni–S(1)	178.09(8)	Ni–S(4)–C(5)	112.3(3)
Cl–Ni–S(4)	90.93(7)	Ni–S(8)–C(7)	106.9(3)
Cl–Ni–S(8)	94.13(7)	Ni–S(8)–C(9)	99.1(3)
Cl–Ni–S(11)	89.95(7)	Ni–S(11)–C(10)	101.0(3)
S(1)–Ni–S(4)	87.28(7)	Ni–S(11)–C(12)	112.3(3)
S(1)–Ni–S(8)	85.28(7)	C(2)–S(1)–C(14)	106.1(4)
S(1)–Ni–S(11)	91.83(7)	S(1)–C(2)–C(3)	105.9(6)
S(1)–Ni–Cl′	94.99(7)	C(2)–C(3)–S(4)	107.9(6)
S(4)–Ni–S(8)	91.45(7)	C(3)–S(4)–C(5)	104.5(4)
S(4)–Ni–S(11)	178.70(8)	S(4)–C(5)–C(6)	120.8(6)
S(4)–Ni–Cl′	90.47(7)	C(5)–C(6)–C(7)	116.8(7)
S(8)–Ni–S(11)	87.53(7)	C(6)–C(7)–S(8)	108.3(6)
S(8)–Ni–Cl′	178.07(7)	C(7)–S(8)–C(9)	106.0(4)
S(11)–Ni–Cl′	90.55(7)	S(8)–C(9)–C(10)	106.6(5)
Cl–Ni–Cl′	85.65(7)	C(9)–C(10)–S(11)	109.2(5)
Ni–Cl–Ni′	94.35(7)	C(10)–S(11)–C(12)	104.9(4)
Ni–S(1)–C(2)	99.3(3)	S(11)–C(12)–C(13)	120.5(6)
Ni–S(1)–C(14)	108.2(3)	C(12)–C(13)–C(14)	117.9(8)
Ni–S(4)–C(3)	101.4(3)	S(1)–C(14)–C(13)	107.6(6)

C(14)–S(1)–C(2)–C(3)	167.3(5)
C(2)–S(1)–C(14)–C(13)	−179.2(6)
S(1)–C(2)–C(3)–S(4)	−68.9(6)
C(2)–C(3)–S(4)–C(5)	161.6(6)
C(3)–S(4)–C(5)–C(6)	−67.6(7)
S(4)–C(5)–C(6)–C(7)	−63.1(9)
C(5)–C(6)–C(7)–S(8)	81.5(8)
C(6)–C(7)–S(8)–C(9)	178.9(5)
C(7)–S(8)–C(9)–C(10)	164.7(5)
S(8)–C(9)–C(10)–S(11)	−68.0(6)
C(9)–C(10)–S(11)–C(12)	161.0(5)
C(10)–S(11)–C(12)–C(13)	−66.7(8)
S(11)–C(12)–C(13)–C(14)	−64.9(10)
C(12)–C(13)–C(14)–S(1)	80.5(8)

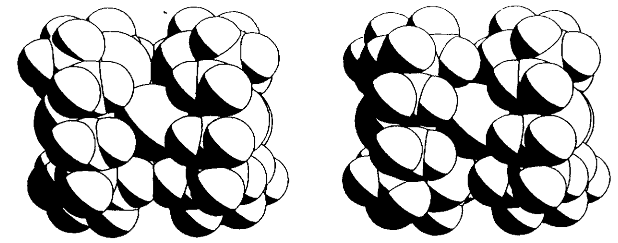

Fig. 4 Space-filling diagram of $[Ni_2([16]aneS_4)_2Cl_2]^{2+}$: (*a*) calculated centrosymmetric model, (*b*) observed structure

$[Ni_2([12]aneS_4)_2Cl_2]^{2+}$ and $[Ni_2([14]aneS_4)_2Cl_2]^{2+}$. The internal angles about the Ni atoms in $[Ni_2([16]aneS_4)_2Cl_2]^{2+}$ approximate to an ideal octahedral geometry [*trans*-S–Ni–Cl 174.40(8)–176.22(7), *trans*-S–Ni–S 178.50(9) and 179.20(8)°], although the conformation of the $[16]aneS_4$ ligand is extremely distorted, with many unfavourable torsion angles of less than 50° within the macrocyclic ring (Table 3); $[Ni_2([16]aneS_4)_2Cl_2]^{2+}$ appears to be the first reported structurally characterised complex of $[16]aneS_4$ to show *cis*-octahedral coordination at a metal centre.[4] The increased absorption

Table 3 Bond lengths (Å), angles and torsion angles (°) with e.s.d.s for $[Ni_2([16]aneS_4)_2Cl_2][BF_4]_2\cdot2MeNO_2$

Ni(1)···Ni(2)	3.5534(12)	C(10)–C(11)	1.529(12)	Ni(2)–Cl(2)	2.4205(20)	C(26)–C(27)	1.505(12)
Ni(1)–S(1)	2.4309(23)	C(11)–C(12)	1.518(12)	S(1)–C(2)	1.835(8)	C(27)–C(28)	1.557(12)
Ni(1)–S(5)	2.4166(23)	C(12)–S(13)	1.815(8)	S(1)–C(16)	1.831(9)	C(28)–S(29)	1.822(9)
Ni(1)–S(9)	2.4259(24)	S(13)–C(14)	1.831(9)	C(2)–C(3)	1.510(11)	S(29)–C(30)	1.815(8)
Ni(1)–S(13)	2.4388(25)	C(14)–C(15)	1.523(12)	C(3)–C(4)	1.540(12)	C(30)–C(31)	1.524(12)
Ni(1)–Cl(1)	2.4182(23)	C(15)–C(16)	1.518(12)	C(4)–S(5)	1.837(8)	C(31)–C(32)	1.527(12)
Ni(1)–Cl(2)	2.4118(22)	S(21)–C(22)	1.821(9)	S(5)–C(6)	1.819(8)	C(32)–S(33)	1.822(9)
Ni(2)–S(21)	2.4421(22)	S(21)–C(36)	1.813(9)	C(6)–C(7)	1.535(12)	S(33)–C(34)	1.813(9)
Ni(2)–S(25)	2.4321(21)	C(22)–C(23)	1.533(13)	C(7)–C(8)	1.519(12)	C(34)–C(35)	1.536(13)
Ni(2)–S(29)	2.4098(22)	C(23)–C(24)	1.521(13)	C(8)–S(9)	1.814(8)	C(35)–C(36)	1.505(13)
Ni(2)–S(33)	2.4258(22)	C(24)–S(25)	1.840(9)	S(9)–C(10)	1.824(8)		
Ni(2)–Cl(1)	2.3860(21)	S(25)–C(26)	1.828(9)				
Cl(1)–Ni(1)–Cl(2)	84.71(7)	C(4)–S(5)–C(6)	95.2(4)	Cl(2)–Ni(2)–S(21)	89.59(7)	C(22)–C(23)–C(24)	115.2(7)
Cl(1)–Ni(1)–S(1)	89.55(8)	S(5)–C(6)–C(7)	113.0(6)	Cl(2)–Ni(2)–S(25)	91.04(7)	C(23)–C(24)–S(25)	112.5(6)
Cl(1)–Ni(1)–S(5)	89.90(8)	C(6)–C(7)–C(8)	116.1(7)	Cl(2)–Ni(2)–S(29)	90.48(7)	Ni(2)–S(25)–C(24)	102.7(3)
Cl(1)–Ni(1)–S(9)	91.77(8)	C(7)–C(8)–S(9)	117.4(6)	Cl(2)–Ni(2)–S(33)	176.09(7)	Ni(2)–S(25)–C(26)	107.5(3)
Cl(1)–Ni(1)–S(13)	175.59(9)	Ni(1)–S(9)–C(8)	110.3(3)	S(21)–Ni(2)–S(25)	88.70(7)	C(24)–S(25)–C(26)	96.4(4)
Cl(2)–Ni(1)–S(1)	90.11(8)	Ni(1)–S(9)–C(10)	103.9(3)	S(21)–Ni(2)–S(29)	179.20(8)	S(25)–C(26)–C(27)	114.3(6)
Cl(2)–Ni(1)–S(5)	174.40(8)	C(8)–S(9)–C(10)	100.5(4)	S(21)–Ni(2)–S(33)	90.24(7)	C(26)–C(27)–C(28)	114.9(7)
Cl(2)–Ni(1)–S(9)	90.72(8)	S(9)–C(10)–C(11)	111.0(6)	S(25)–Ni(2)–S(29)	90.50(7)	C(27)–C(28)–S(29)	116.5(6)
Cl(2)–Ni(1)–S(13)	90.88(8)	C(10)–C(11)–C(12)	114.2(7)	S(25)–Ni(2)–S(33)	92.87(7)	Ni(2)–S(29)–C(28)	110.1(3)
S(1)–Ni(1)–S(5)	88.32(8)	C(11)–C(12)–S(13)	111.6(6)	S(29)–Ni(2)–S(33)	89.74(7)	Ni(2)–S(29)–C(30)	104.5(3)
S(1)–Ni(1)–S(9)	178.50(9)	Ni(1)–S(13)–C(12)	102.9(3)	Ni(1)–Cl(1)–Ni(2)	95.40(8)	C(28)–S(29)–C(30)	101.0(4)
S(1)–Ni(1)–S(13)	90.55(8)	Ni(1)–S(13)–C(14)	107.8(3)	Ni(1)–Cl(2)–Ni(2)	94.67(7)	S(29)–C(30)–C(31)	110.8(6)
S(5)–Ni(1)–S(9)	90.96(8)	C(12)–S(13)–C(14)	97.2(4)	Ni(1)–S(1)–C(2)	105.3(3)	C(30)–C(31)–C(32)	115.7(7)
S(5)–Ni(1)–S(13)	94.51(8)	S(13)–C(14)–C(15)	112.9(6)	Ni(1)–S(1)–C(16)	110.8(3)	C(31)–C(32)–S(33)	112.6(6)
S(9)–Ni(1)–S(13)	88.19(8)	C(14)–C(15)–C(16)	116.5(7)	C(2)–S(1)–C(16)	100.1(4)	Ni(2)–S(33)–C(32)	102.4(3)
Cl(1)–Ni(2)–Cl(2)	85.21(7)	S(1)–C(16)–C(15)	117.2(6)	S(1)–C(2)–C(3)	110.2(5)	Ni(2)–S(33)–C(34)	107.2(3)
Cl(1)–Ni(2)–S(21)	90.81(7)	Ni(2)–S(21)–C(22)	104.8(3)	C(2)–C(3)–C(4)	115.8(7)	C(32)–S(33)–C(34)	96.8(4)
Cl(1)–Ni(2)–S(25)	176.22(7)	Ni(2)–S(21)–C(36)	109.9(3)	C(3)–C(4)–S(5)	111.9(6)	S(33)–C(34)–C(35)	115.1(6)
Cl(1)–Ni(2)–S(29)	90.00(7)	C(22)–S(21)–C(36)	100.5(4)	Ni(1)–S(5)–C(4)	103.9(3)	C(34)–C(35)–C(36)	116.5(8)
Cl(1)–Ni(2)–S(33)	90.88(7)	S(21)–C(22)–C(23)	110.7(6)	Ni(1)–S(5)–C(6)	106.5(3)	S(21)–C(36)–C(35)	117.7(6)
C(16)–S(1)–C(2)–C(3)	163.3(6)	S(9)–C(10)–C(11)–C(12)	45.6(8)	C(24)–S(25)–C(26)–C(27)	173.5(6)		
C(2)–S(1)–C(16)–C(15)	55.3(7)	C(10)–C(11)–C(12)–S(13)	45.1(8)	S(25)–C(26)–C(27)–C(28)	−77.3(8)		
S(1)–C(2)–C(3)–C(4)	47.3(8)	C(11)–C(12)–S(13)–C(14)	165.7(6)	C(26)–C(27)–C(28)–S(29)	72.0(9)		
C(2)–C(3)–C(4)–S(5)	40.7(9)	C(12)–S(13)–C(14)–C(15)	174.2(6)	C(27)–C(28)–S(29)–C(30)	51.1(7)		
C(3)–C(4)–S(5)–C(6)	169.8(6)	S(13)–C(14)–C(15)–C(16)	−78.5(8)	C(28)–S(29)–C(30)–C(31)	164.7(6)		
C(4)–S(5)–C(6)–C(7)	176.0(6)	C(14)–C(15)–C(16)–S(1)	71.2(9)	S(29)–C(30)–C(31)–C(32)	46.3(9)		
S(5)–C(6)–C(7)–C(8)	−78.8(8)	C(36)–S(21)–C(22)–C(23)	164.6(6)	C(30)–C(31)–C(32)–S(33)	43.2(9)		
C(6)–C(7)–C(8)–S(9)	70.1(9)	C(22)–S(21)–C(36)–C(35)	52.4(7)	C(31)–C(32)–S(33)–C(34)	169.1(6)		
C(7)–C(8)–S(9)–C(10)	54.1(7)	S(21)–C(22)–C(23)–C(24)	45.4(9)	C(32)–S(33)–C(34)–C(35)	172.6(7)		
C(8)–S(9)–C(10)–C(11)	163.1(6)	C(22)–C(23)–C(24)–S(25)	44.2(9)	S(33)–C(34)–C(35)–C(36)	−75.5(9)		
		C(23)–C(24)–S(25)–C(26)	167.4(6)	C(34)–C(35)–C(36)–S(21)	69.6(9)		

coefficients in the electronic spectrum of this complex compared to those for the [12]aneS_4 and [14]aneS_4 dimers suggests that the non-centrosymmetric structure observed in the solid state may be retained in solution {for $[Ni_2L_2Cl_2][BF_4]_2$, L = [12]aneS_4, λ_{max} = 288 (ε_{max} = 407) and 244 (4125); for L = [14]aneS_4, λ_{max} = 284 (ε_{max} = 922) and 244 (4670); for L = [16]aneS_4, λ_{max} = 312 (ε_{max} = 8520) and 256 nm (7180 $dm^3 mol^{-1} cm^{-1}$)}.

The above *cis*-octahedral complexes $[Ni_2L_2(\mu\text{-}Cl)_2]^{2+}$ (L = [14]aneS_4 or [16]aneS_4) contrast with the previously reported structures of the square-planar $[Ni([14]aneS_4)]^{2+}$ (ref. 9) and *trans*-octahedral $[Ni([16]aneS_4)(OH_2)_2]^{2+}$,[7] in which the Ni is surrounded by a coplanar array of S-donor atoms.

Heating a solution of $[Ni_2([14]aneS_4)_2Cl_2][BF_4]_2$ in $MeNO_2$ to 60 °C caused its rapid conversion into the red square-planar complex $[Ni([14]aneS_4)]^{2+}$.[8] In contrast, no reaction was observed on heating $[Ni_2L_2Cl_2][BF_4]_2$ (L = [12]aneS_4 or [16]aneS_4) in $MeNO_2$, the dimers being recovered unchanged. Similarly, treatment of $[Ni_2([14]aneS_4)_2Cl_2][BF_4]_2$ with Tl^+ in $MeNO_2$ at 293 K afforded $[Ni([14]aneS_4)]^{2+}$ in quantitative yield, whilst analogous reactions for L = [12]aneS_4 and [16]aneS_4 resulted in decomposition with no nickel(II) macrocyclic species being isolable. This demonstrates both the poorer metal ion–hole size fit between Ni^{II} and [12]- and [16]-aneS_4, and the stability of the dichloro-bridged bioctahedral structures $[Ni_2L_2Cl_2]^{2+}$ in the absence of competing ligands.

Cyclic voltammetry of the complexes $[Ni_2L_2Cl_2][BF_4]_2$ in MeCN–0.1 mol dm^{-3} $NBu^n_4BF_4$ at 293 K yielded complex results. The complex $[Ni_2([12]aneS_4)_2Cl_2]^{2+}$ exhibits an irreversible oxidation at E_{pa} = +1.06 V *vs.* ferrocene–ferrocenium (scan rate 400 mV s^{-1}), together with a weak return wave at E_{pc} = +0.14 V due to an unstable daughter product. An irreversible reduction is also observed at E_{pc} = −1.39 V, with an approximately equal-intensity return wave at E_{pa} = −0.31 V. On addition of a ten-fold excess of NBu^n_4Cl the cyclic voltammogram changes to show irreversible waves at E_{pa} = +0.82 V and E_{pc} = −1.98 V, with no observable daughter products. In contrast, $[Ni_2([14]aneS_4)_2Cl_2]^{2+}$ and $[Ni_2([16]aneS_4)_2Cl_2]^{2+}$ each show two irreversible oxidations at E_{pa} = +0.78, +1.25 and E_{pa} = +0.72, +1.21 V respectively. Addition of a ten-fold excess of NBu^n_4Cl causes the first of these oxidations to become quasi-reversible at $E_{\frac{1}{2}}$ = +0.60 V, ΔE = *ca.* 340 mV for both complexes, whilst the second wave is reduced in intensity relative to the first. No reduction waves were observed for these two complexes. All of the above processes remained irreversible at high scan rates. Attempts to electrogenerate bulk samples of the redox products described

Table 4 Atomic coordinates with e.s.d.s for $[Ni_2([12]aneS_4)_2Cl_2][BF_4]_2\cdot 2MeNO_2$

Atom	x	y	z
Ni	0.378 42(12)	0.000 0	0.377 65(12)
S(1)	0.153 0(3)	0.000 0	0.327 42(25)
C(2)	0.132 4(8)	0.107 5(6)	0.405 5(7)
C(3)	0.188 9(8)	0.195 7(6)	0.356 5(7)
S(4)	0.353 79(20)	0.177 57(15)	0.362 40(18)
C(5)	0.353 2(9)	0.194 2(6)	0.218 6(7)
C(6)	0.300 2(9)	0.107 5(6)	0.146 1(7)
S(7)	0.395 6(3)	0.000 0	0.195 52(24)
Cl	0.603 75(24)	0.000 0	0.431 74(23)
C(1S)	−0.256 4(14)	0.000 0	0.139 0(12)
N(1S)	−0.201 2(10)	0.000 0	0.255 3(10)
O(1S)	−0.178 5(7)	0.078 0(5)	0.302 9(6)
B(1)	0.500 0	0.273 7(11)	0.000 0
F(1)	0.452 4(8)	0.335 5(5)	0.065 1(6)
F(2)	0.411 1(7)	0.220 7(6)	−0.062 4(6)

Table 5 Atomic coordinates with e.s.d.s for $[Ni_2([14]aneS_4)_2Cl_2][BF_4]\cdot 6MeNO_2$

Atom	x	y	z
Ni	0.151 07(8)	0.997 59(7)	0.031 89(7)
Cl	0.116 30(17)	0.908 74(15)	−0.127 46(15)
S(1)	0.187 64(19)	1.077 13(17)	0.188 34(16)
C(2)	0.117 2(9)	0.987 3(7)	0.304 7(7)
C(3)	0.205 9(8)	0.849 6(7)	0.249 7(7)
S(4)	0.150 51(19)	0.821 24(16)	0.132 83(16)
C(5)	0.298 6(8)	0.678 1(7)	0.042 2(7)
C(6)	0.450 7(8)	0.674 7(7)	−0.031 3(7)
C(7)	0.465 1(8)	0.755 4(7)	−0.130 3(7)
S(8)	0.412 88(18)	0.911 46(16)	−0.065 61(16)
C(9)	0.436 7(8)	1.004 1(6)	−0.191 2(6)
C(10)	0.354 9(8)	1.139 0(6)	−0.136 8(6)
S(11)	0.156 51(19)	1.173 88(15)	−0.068 59(16)
C(12)	0.077 8(9)	1.314 5(7)	0.034 3(7)
C(13)	0.111 8(9)	1.314 1(8)	0.143 0(7)
C(14)	0.058 0(9)	1.237 0(7)	0.238 2(7)
B	0.361 8(10)	0.456 8(8)	−0.237 3(8)
F(1)	0.481 9(9)	0.353 4(7)	−0.275 7(9)
F(2)	0.378 4(14)	0.558 6(7)	−0.250 0(8)
F(3)	0.300 0(11)	0.450 2(7)	−0.121 5(6)
F(4)	0.281(3)	0.473 0(22)	−0.298 8(23)
F(5)	0.409(4)	0.439(3)	−0.361 1(23)
F(6)	0.245 5(18)	0.429 4(16)	−0.241 2(17)
C(1S)	0.193 6(15)	0.227 1(12)	0.624 7(11)
N(1S)	0.184 7(12)	0.197 3(8)	0.517 1(9)
O(1SA)	0.279 6(11)	0.207 3(12)	0.421 6(8)
O(1SB)	0.072 2(10)	0.191 6(8)	0.526 3(8)
C(2S)	0.241 9(12)	0.552 9(10)	−0.549 9(10)
N(2S)	0.192 0(14)	0.505 1(10)	−0.620 9(11)
O(2SA)	0.194 9(11)	0.525 7(10)	−0.710 6(8)
O(2SB)	0.258 2(19)	0.380 0(18)	−0.625 6(14)
O(2SC)	0.065 5(25)	0.482 2(23)	−0.545 4(20)
C(3S)	0.417 1(12)	−0.256 9(10)	0.567 8(9)
N(3S)	0.346 9(10)	−0.161 2(8)	0.509 8(9)
O(3SA)	0.229 6(8)	−0.160 2(7)	0.509 1(7)
O(3SB)	0.405 1(14)	−0.097 5(10)	0.460 3(16)

above resulted in diamagnetic solutions and/or nickel metal deposition onto the platinum working electrode, demonstrating the instability of the oxidised and reduced species. Hence, on the basis of cyclic voltammetric data, no assignment of the redox processes observed for the $[Ni_2L_2Cl_2]^{2+}$ dimers can be made. In particular, it is unclear whether the observed oxidations are metal based, or arise from the oxidation of free chloride [$E(Cl^-–Cl) = +1.0$ V] released by dissociation of the dimeric complexes in solution. However, since the cyclic voltammograms of $[Ni_2L_2Cl_2]^{2+}$ differ from those of the analogous monomeric complexes $[NiL(solv)_2]^{2+}$ measured under identical conditions,[7] it is unlikely that complete dissociation of the dimeric complexes occurs in MeCN solution. It is possible that the reduction observed for $[Ni_2([12]aneS_4)_2Cl_2]^{2+}$ may correspond to the formation of a metal–metal bonded nickel(I) dimer[23] analogous to those observed in the electrochemical reduction of $[PdL]^{2+}$ (L = [12]aneS$_4$, [14]aneS$_4$ or [16]-aneS$_4$).[4,24] Nickel–nickel bond formation might be expected to be less favoured for the other dimers, since close approach of the two nickel ions would be hindered by steric interactions between the macrocyclic rings (see above).

Treatment of $NiCl_2$ with 1 molar equivalent of [9]aneS$_3$ and $NaBF_4$ under identical conditions to those described above afforded a pale green solution, from which a green solid could be isolated on addition of Et_2O. Fractional recrystallisation of this crude product from MeCN–Et_2O yielded an approximate 1:2 mixture of the known pink $[Ni([9]aneS_3)_2][BF_4]_2$[11] and a pale green compound, the latter being obtained in 45% final yield. On the basis of mass spectral and microanalytical data, the green product was formulated as the face-sharing bioctahedral dimeric complex $[Ni_2([9]aneS_3)_2(\mu\text{-}Cl)_3]BF_4$. This assignment was confirmed by a single-crystal X-ray analysis of $[Ni_2([9]aneS_3)_2(\mu\text{-}Cl)_3]BF_4\cdot MeCN$, the details of which have been reported elsewhere.[25]

Experimental

Infrared spectra were run as KBr discs on a Perkin-Elmer 598 spectrometer over the range 200–4000 cm^{-1}, electronic spectra for solutions in 1 cm quartz cells using a Perkin-Elmer Lambda 9 spectrophotometer and fast-atom bombardment (FAB) mass spectra on a Kratos MS 50TC spectrometer using a 3-nitrobenzyl alcohol matrix. Microanalyses were carried out by the University of Edinburgh Chemistry Department microanalytical service. Electrochemical measurements were performed usng a Bruker E310 universal modular polarograph; for all readings a three-electrode system in acetonitrile containing 0.1 mol dm^{-3} $NBu^n{}_4PF_6$ as supporting electrolyte was employed. Cyclic voltammetric measurements were obtained with a double platinum electrode and a Ag–AgCl reference electrode. Potentials are quoted *versus* ferrocene–ferrocenium, at a scan rate of 400 mV s^{-1}. Anhydrous $NiCl_2$ was prepared by dehydration of $NiCl_2\cdot 6H_2O$ at 393 K for 2 weeks.

Syntheses.—$[Ni_2([12]aneS_4)_2(\mu\text{-}Cl)_2][BF_4]_2$. Reaction of anhydrous $NiCl_2$ (0.021 g, 1.6 × 10^{-4} mol) with [12]aneS$_4$ (0.036 g, 1.6 × 10^{-4} mol) in $MeNO_2$ (4 cm^3) at 293 K for 30 min afforded a pale green precipitate. Addition of $NaBF_4$ (0.018 g, 1.6 × 10^{-4} mol) and heating the resultant mixture to 40 °C caused this precipitate to dissolve, yielding a green solution and a white precipitate of NaCl. The solution was filtered, reduced to 1 cm^3 in volume and the green solid product crystallised by the addition of an excess of Et_2O. The complex was recrystallised from $MeNO_2$–Et_2O. Yield 0.046 g, 68% (Found: C, 22.5; H, 3.8. Calc. for $C_{16}H_{32}B_2Cl_2F_8Ni_2S_8$: C, 22.8; H, 3.8%). Electronic spectrum (in MeCN): λ_{max} = 980 (ε_{max} = 26), 608 (31), 384 (93), 288 (407) and 244 nm (4125 dm^3 mol^{-1} cm^{-1}). IR: 2960m, 2920m, 2840w, 1425s, 1410s, 1300m, 1255s, 1205s, 1180w, 1060vs, 1030w, 990w, 915m, 895w, 850m, 840w, 820m, 800m, 770w, 675w, 655w, 525s and 425w cm^{-1}.

$[Ni_2([14]aneS_4)_2(\mu\text{-}Cl)_2][BF_4]_2$. Method as above, using [14]aneS$_4$ (0.040 g, 1.6 × 10^{-4} mol). The product was isolated as a pale blue microcrystalline solid. Yield 0.045 g, 62% (Found: C, 26.7; H, 4.4. Calc. for $C_{20}H_{40}B_2Cl_2F_8Ni_2S_8$: C, 26.7; H, 4.5%). FAB mass spectrum: found m/z = 809, 722, 361 and 326; calc. for $[^{58}Ni_2([14]aneS_4)_2{}^{35}Cl_2(^{11}BF_4)]^+$ m/z 809, $[^{58}Ni_2([14]aneS_4)_2{}^{35}Cl_2]^+$ 722, $[^{58}Ni([14]aneS_4)^{35}Cl]^+$ 361 and $[^{58}Ni([14]aneS_4)]^+$ 326 with correct isotopic distributions. Electronic spectrum (in MeCN): λ_{max} = 915 (ε_{max} = 36), 598 (26), 380 (sh), 284 (922) and 244 nm (4670 dm^3 mol^{-1} cm^{-1}). IR: 2950m, 2910m, 2840w, 1400s, 1305m, 1255w, 1245m, 1195w,

Table 6 Atomic coordinates with e.s.d.s for $[Ni_2([16]aneS_4)_2Cl_2][BF_4]_2 \cdot 2MeNO_2$

Atom	*x*	*y*	*z*	Atom	*x*	*y*	*z*
Ni(1)	0.190 28(7)	0.665 11(7)	−0.001 49(6)	S(29)	0.051 03(12)	0.911 00(15)	−0.082 72(12)
Ni(2)	0.000 0	0.798 30(7)	0.000 0	C(30)	−0.041 8(5)	0.972 6(6)	−0.116 3(4)
Cl(1)	0.056 18(12)	0.665 13(14)	−0.061 71(11)	C(31)	−0.086 9(5)	0.910 0(6)	−0.170 0(5)
Cl(2)	0.134 14(12)	0.800 59(13)	0.060 39(11)	C(32)	−0.098 6(5)	0.802 6(6)	−0.151 5(4)
S(1)	0.135 44(12)	0.551 87(14)	0.080 75(11)	S(33)	−0.131 19(13)	0.786 29(15)	−0.064 69(12)
C(2)	0.199 8(5)	0.441 5(6)	0.074 6(4)	C(34)	−0.156 8(5)	0.657 6(7)	−0.071 8(5)
C(3)	0.169 0(5)	0.379 3(6)	0.015 7(4)	C(35)	−0.178 0(6)	0.607 3(7)	−0.005 0(5)
C(4)	0.152 2(5)	0.433 7(6)	−0.051 8(4)	C(36)	−0.105 7(5)	0.584 4(7)	0.043 1(4)
S(5)	0.232 69(12)	0.525 84(14)	−0.067 22(11)	B(1)	0.078 0(6)	0.261 9(7)	0.179 8(5)
C(6)	0.198 2(5)	0.549 9(6)	−0.154 4(4)	F(11)	0.154 9(4)	0.227 5(5)	0.163 4(4)
C(7)	0.247 6(5)	0.632 3(6)	−0.187 5(4)	F(12)	0.031 1(4)	0.270 4(6)	0.121 5(4)
C(8)	0.223 1(5)	0.735 8(6)	−0.168 8(4)	F(13)	0.089 4(4)	0.350 1(5)	0.211 4(4)
S(9)	0.248 63(13)	0.776 35(15)	−0.082 98(11)	F(14)	0.041 3(5)	0.196 6(6)	0.220 9(4)
C(10)	0.360 3(5)	0.750 5(6)	−0.077 6(4)	B(2)	0.588 9(6)	0.262 4(8)	0.321 4(5)
C(11)	0.402 8(5)	0.805 3(6)	−0.018 3(4)	F(21)	0.547 0(8)	0.342 8(7)	0.300 0(6)
C(12)	0.356 6(5)	0.799 4(6)	0.047 4(4)	F(22)	0.558 0(9)	0.174 2(7)	0.308 8(6)
S(13)	0.321 78(14)	0.675 84(15)	0.064 21(12)	F(23)	0.636 3(16)	0.286 6(9)	0.374 9(9)
C(14)	0.297 2(5)	0.694 2(6)	0.153 2(4)	F(24)	0.668 4(10)	0.246 3(22)	0.321 2(14)
C(15)	0.256 3(5)	0.605 3(6)	0.184 5(4)	F(25)	0.550 6(16)	0.256 2(23)	0.379 4(14)
C(16)	0.164 1(5)	0.590 2(6)	0.167 4(4)	F(26)	0.623 3(15)	0.270 7(22)	0.259 7(13)
S(21)	−0.052 52(13)	0.686 01(15)	0.084 70(12)	C(1S)	0.469 2(7)	−0.005 8(9)	0.258 3(6)
C(22)	−0.140 7(5)	0.749 4(6)	0.120 4(4)	N(1S)	0.408 0(5)	0.051 8(5)	0.290 6(4)
C(23)	−0.110 6(6)	0.823 1(7)	0.174 4(5)	O(1SA)	0.368 6(4)	0.110 7(5)	0.255 8(4)
C(24)	−0.037 2(5)	0.886 3(6)	0.154 9(4)	O(1SB)	0.395 2(7)	0.039 7(6)	0.349 0(4)
S(25)	−0.049 04(13)	0.933 71(14)	0.067 77(11)	C(2S)	0.681 7(7)	0.506 7(9)	0.249 0(6)
C(26)	0.035 4(5)	1.023 2(6)	0.075 1(4)	N(2S)	0.743 4(7)	0.463 4(9)	0.206 4(10)
C(27)	0.054 5(5)	1.073 7(7)	0.009 6(5)	O(2SA)	0.744 4(8)	0.485 7(12)	0.148 3(8)
C(28)	0.105 8(5)	1.011 8(6)	−0.040 3(4)	O(2SB)	0.792 5(7)	0.405 8(8)	0.235 1(9)

1155w, 1060vs, 1030w, 980w, 920m, 865s, 845m, 810w, 800w, 770w, 690w, 655w, 525s and 460w cm^{-1}.

$[Ni_2([16]aneS_4)_2(\mu\text{-}Cl)_2][BF_4]_2$. Method as above, using $[16]aneS_4$ (0.044 g, 1.6×10^{-4} mol). The complex was isolated as a green microcrystalline solid. Yield 0.052 g, 73% (Found: C, 29.8; H, 5.1. Calc. for $C_{24}H_{48}B_2Cl_2F_8Ni_2S_8$: C, 30.2; H, 5.0%). FAB mass spectrum: found m/z = 778, 389 and 354; calc. for $[^{58}Ni_2([16]aneS_4)_2{}^{35}Cl_2]^+$ m/z = 778, $[^{58}Ni([16]aneS_4)\text{-}{}^{35}Cl]^+$ 389 and $[^{58}Ni([16]aneS_4)]^+$ 354 with correct isotopic distributions. Electronic spectrum (in MeCN): λ_{max} = 970 (ε_{max} = 19), 566 (33), 370 (sh), 312 (8520) and 256 nm (7180 dm^3 mol^{-1} cm^{-1}). IR: 2900s, 2840m, 1440s, 1425s, 1290s, 1250m, 1245m, 1190w, 1145w, 1060vs, 990w, 945w, 930w, 880s, 840m, 770s, 720w, 695w, 650w, 525s and 460w cm^{-1}.

$[Ni_2([9]aneS_3)_2(\mu\text{-}Cl)_3]BF_4$. Method as above, using $[9]\text{-}aneS_3$ (0.030 g, 1.6×10^{-4} mol). The product was isolated as a pale green microcrystalline product. Yield 0.025 g, 45% (Found: C, 21.5; H, 3.7. Calc. for $C_{12}H_{24}BCl_3F_4Ni_2S_6$: C, 21.5; H, 3.6%). FAB mass spectrum: found m/z = 581, 546 and 238; calc. for $[^{58}Ni_2([9]aneS_3)_2{}^{35}Cl_3]^+$ m/z = 581, $[^{58}Ni_2([9]\text{-}aneS_3)_2{}^{35}Cl_2]^+$ 546 and $[^{58}Ni([9]aneS_3)]^+$ 238 with correct isotopic distributions. Electronic spectrum (in MeCN): λ_{max} = 1026 (ε_{max} = 80), 653 (37), 352 (sh), 286 (9150) and 256 nm (6770 dm^3 mol^{-1} cm^{-1}). IR: 2950m, 2920m, 2840w, 1445s, 1410s, 1380w, 1300m, 1280m, 1255w, 1060vs, 930m, 900m, 825m, 765w, 720w, 700w, 670w, 620w, 550w, 525m, 470w and 430m cm^{-1}.

Single-crystal Structure Determinations.—Single crystals of $[Ni_2L_2Cl_2][BF_4]_2 \cdot n MeNO_2$ (L = $[12]aneS_4$, n = 2; $[14]\text{-}aneS_4$, 6; or $[16]aneS_4$, 2) were obtained by diffusion of Et_2O vapour into $MeNO_2$ solutions of the complexes. For L = $[12]aneS_4$ and $[16]aneS_4$ a single crystal was selected and to prevent solvent loss was placed in a 0.5 mm capillary tube, which was then mounted on a Stoë Stadi-4 four-circle diffractometer equipped with an Oxford Cryosystems low-temperature device[26] and employing Mo-Kα radiation (λ = 0.710 73 Å). For L = $[14]aneS_4$, a suitable crystal was cooled in mother-liquor over solid CO_2 whilst being mounted on a glass fibre, then cooled to 173 K as above. Structure-factor data were inlaid[27] or taken from ref. 28. Illustrations were prepared using SHELXTL/PC[29] and molecular geometry calculations performed using CALC.[30] Crystallographic data for the structure determinations are listed in Table 7.

$[Ni_2([12]aneS_4)_2Cl_2][BF_4]_2 \cdot 2MeNO_2$. A Patterson search conducted using the ORIENT and TRADIR routines of DIRDIF[31] located the NiS_4Cl input fragment and iterative rounds of least-squares refinement and Fourier difference synthesis[27] located all other non-H atoms. At isotropic convergence, an empirical absorption correction was made using DIFABS[32] (maximum and minimum corrections 1.185 and 0.691). Anisotropic thermal parameters were refined for all non-H atoms, and H atoms were refined in fixed, calculated positions.

$[Ni_2([14]aneS_4)_2Cl_2][BF_4]_2 \cdot 6MeNO_2$. After difficulties were encountered trying to solve the structure in the most likely triclinic space group $P\bar{1}$ a solution was obtained in the space group $P1$ using automatic direct methods[33] and developed by least-squares refinement and Fourier difference synthesis.[27] After an initial refinement an examination of the correlation-matrix elements suggested that atomic parameters were not all independent and that additional symmetry was present. After remerging the data and shifting the origin so that a crystallographic inversion centre lay at the midpoint of the Ni • • • Ni vector, a further refinement was successfully carried out in the space group $P\bar{1}$. During refinement, the BF_4^- counter ion and one $MeNO_2$ were found to be disordered and were modelled using partially occupied F and O atoms respectively. Anisotropic thermal parameters were refined for all Ni, S, Cl, N, F and O atoms with site occupancy > 0.5 and H atoms were included in fixed, calculated positions.

$[Ni_2([16]aneS_4)_2Cl_2][BF_4]_2 \cdot 2MeNO_2$. The nickel positions were deduced from a Patterson synthesis[33] and iterative cycles of least-squares refinement and Fourier difference synthesis[27] located the other non-H atoms. During refinement one BF_4^- counter ion was found to be disordered; this was modelled using partially occupied F atoms, such that the total number of

Table 7 Crystallographic data for $[Ni_2L_2Cl_2][BF_4]_2 \cdot nMeNO_2$

L, *n*	[12]aneS_4, 2	[14]aneS_4, 6	[16]aneS_4, 2
Molecular formula	$C_{18}H_{38}B_2Cl_2F_8N_2Ni_2O_4S_8$	$C_{26}H_{58}B_2Cl_2F_8N_6Ni_2O_{12}S_8$	$C_{26}H_{54}B_2Cl_2F_8N_2Ni_2O_4S_8$
M_r	964.82	1 265.05	1 077.04
System	Monoclinic	Triclinic	Monoclinic
Space group	$C2/m$	$P\bar{1}$	Cc
a/Å	11.0651(20)	10.6341(18)	16.024(4)
b/Å	13.4977(24)	11.6841(22)	13.6862(17)
c/Å	12.7222(21)	12.2457(25)	19.7329(24)
α/°	90	88.547(7)	90
β/°	104.824(21)	67.288(12)	92.042(19)
γ/°	90	68.647(6)	90
U/Å^3	1 836.9	1 295.4	4 324.8
Z	2	1	4
D_c/g cm^{-3}	1.744	1.621	1.654
Crystal appearance	Green plate	Blue column	Green plate
Crystal dimensions/mm	0.39 × 0.27 × 0.06	0.77 × 0.23 × 0.17	0.60 × 0.35 × 0.25
μ(Mo-Kα)/mm^{-1}	1.683	1.226	1.439
F(000)	984	652	2 224
T/K	295	173	173
Reflections measured	1 266*	3 300	3 925
$2\theta_{max}$/°	45	45	45
h, k, l ranges	−11 to 11, 0–14, 0–13	−10 to 10, −12 to 12, 0–13	−17 to 17, 0–14, 0–21
Reflections observed [$F > 6\sigma(F)$]	809	2 790	2 800
Final R	0.0439	0.0630	0.0373
Final R'	0.0557	0.0742	0.0498
Final S	1.131	1.146	1.158
No. of parameters	119	245	370
Weighting scheme, w^{-1}	$\sigma^2(F) + 0.001\,158F^2$	$\sigma^2(F) + 0.000\,031F^2$	$\sigma^2(F) + 0.000\,041F^2$
Final maximum and minimum electron density/e Å^{-3}	+0.61, −0.44	+1.15, −0.73	+0.41, −0.39

* Crystal decay of 18% noted and corrected for during data collection.

F atoms equalled four. Hydrogen atoms were included in fixed calculated positions. Anisotropic thermal parameters were refined for all atoms except C, B and H.

Additional material available from the Cambridge Crystallographic Data Centre comprises H-atom coordinates, thermal parameters and remaining bond lengths and angles.

Acknowledgements

We thank ICI Colours and Fine Chemicals (Blackley) for a CASE award to M. A. H., the SERC for support, and the Royal Society of Edinburgh and the Scottish Office Education Department for a Support Research Fellowship (to M. S.).

References

1 S. W. Ragsdale, L. G. Ljungdahl and D. V. DerVartanian, *Biochem. Biophys. Res. Commun.*, 1983, **115**, 658; P. A. Lindahl, N. Kojima, R. P. Hausinger, J. A. Fox, B. K. Teo, C. T. Walsh and W. H. Orme-Johnson, *J. Am. Chem. Soc.*, 1984, **106**, 3062; R. A. Scott, S. A. Wallin, M. Czechowski, D. V. DerVartanian, J. LeGall, H. D. Peck, jun. and I. Moura, *J. Am. Chem. Soc.*, 1984, **106**, 6864; R. Cammack, *Adv. Inorg. Chem.*, 1988, **32**, 197 and refs. therein.

2 H.-J. Krüger and R. H. Holm, *Inorg. Chem.*, 1987, **26**, 3645; *Inorg. Chem.*, 1989, **28**, 1148; *J. Am. Chem. Soc.*, 1990, **112**, 2955; H.-J. Krüger, G. Peng and R. H. Holm, *Inorg. Chem.*, 1991, **30**, 734; S. Fox, Y. Wang, A. Silver and M. Millar, *J. Am. Chem. Soc.*, 1990, **112**, 3218; J. D. Franolic, W. Y. Wang and M. Millar, *J. Am. Chem. Soc.*, 1992, **114**, 6587; S. B. Choudhury, D. Ray and A. Chakravorty, *Inorg. Chem.*, 1990, **29**, 4603; 1991, **30**, 4354; *J. Chem. Soc., Dalton Trans.*, 1992, 107; N. Baidya, M. Olmstead and P. K. Mascharak, *Inorg. Chem.*, 1991, **30**, 929; M. Zimmer, G. Schulte, X.-L. Luo and R. H. Crabtree, *Angew. Chem., Int. Ed. Engl.*, 1991, **30**, 193; T. Yamamura, S. Sakurai, H. Arai and H. Miyamae, *J. Chem. Soc., Chem. Commun.*, 1993, 1656.

3 P. Stavropoulos, M. C. Muetterties, M. Carri and R. H. Holm, *J. Am. Chem. Soc.*, 1991, **113**, 8485.

4 M. Schröder, *Pure Appl. Chem.*, 1988, **60**, 517; A. J. Blake and M. Schröder, *Adv. Inorg. Chem.*, 1990, **35**, 1 and refs. therein.

5 M. A. Halcrow, Ph.D. Thesis, University of Edinburgh, 1991; A. J. Blake, R. O. Gould, M. A. Halcrow, A. J. Holder, T. I. Hyde and M. Schröder, *J. Chem. Soc., Dalton Trans.*, 1992, 3427.

6 A. J. Blake, R. O. Gould, M. A. Halcrow and M. Schröder, *J. Chem. Soc., Dalton Trans.*, 1993, 2909.

7 A. J. Blake, M. A. Halcrow and M. Schröder, *J. Chem. Soc., Dalton Trans.*, 1992, 2803.

8 W. Rosen and D. H. Busch, *Chem. Commun.*, 1969, 148; *J. Am. Chem. Soc.*, 1969, **91**, 4694.

9 P. H. Davis, L. K. White and R. L. Belford, *Inorg. Chem.*, 1975, **14**, 1753.

10 W. Rosen and D. H. Busch, *Inorg. Chem.*, 1970, **9**, 262.

11 W. N. Setzer, C. A. Ogle, G. S. Wilson and R. S. Glass, *Inorg. Chem.*, 1983, **22**, 266.

12 S. R. Cooper, S. C. Rawle, J.-A. R. Hartman, E. J. Hintsa and C. A. Admans, *Inorg. Chem.*, 1988, **27**, 1209.

13 L. Sacconi, F. Mani and A. Bencini, in *Comprehensive Coordination Chemistry*, eds. G. Wilkinson, R. D. Gillard and J. A. McCleverty, Pergamon, Oxford, 1987, vol. 5, ch. 50, pp. 45–68 and 276–284 and refs. therein.

14 For recent examples, see Z. Janas, P. Sobota and T. Lis, *J. Chem. Soc., Dalton Trans.*, 1991, 2429; F. A. Cotton and R. C. Torralba, *Inorg. Chem.*, 1991, **30**, 2196, 4386; F. A. Cotton, C. M. Daniels, K. R. Dunbar, C. R. Falvello, C. J. O'Connor and A. C. Price, *Inorg. Chem.*, 1991, **30**, 2509; N. Barba-Behrens, A. M. Mutio-Rico, P. Joseph-Nathan and R. Contreras, *Polyhedron*, 1991, **10**, 1333; W. Clegg, R. J. Errington, R. J. Flynn, M. E. Green, D. C. R. Hockless, N. C. Norman, V. C. Gibson and K. Tavakkoli, *J. Chem. Soc., Dalton Trans.*, 1992, 1753.

15 For example, see R. L. Lintvedt, L. L. Born, D. P. Murtha, J. M. Kuszaj and M. D. Glick, *Inorg. Chem.*, 1974, **13**, 18; G. J. Long and E. O. Schlemper, *Inorg. Chem.*, 1974, **13**, 279; R. J. Butcher and E. Sinn, *Inorg. Chem.*, 1977, **16**, 2334; R. J. Butcher, C. J. O'Connor and E. Sinn, *Inorg. Chem.*, 1981, **20**, 3486.

16 D. M. Duggan, E. K. Barefield and D. N. Hendrickson, *Inorg. Chem.*, 1973, **12**, 985.

17 C. G. Pierpoint, D. N. Hendrickson, D. M. Duggan, F. Wagner and E. K. Barefield, *Inorg. Chem.*, 1975, **14**, 604.

18 P. Chaudhuri, H.-J. Küppers, K. Wieghardt, S. Gehring, W. Haase, B. Nuber and J. Weiss, *J. Chem. Soc., Dalton Trans.*, 1988, 1367.
19 K. O. Joung, C. J. O'Connor, E. Sinn and R. L. Carlin, *Inorg. Chem.*, 1979, **18**, 804.
20 R. Carballo, A. Castiñeiras, W. Hiller and J. Strähle, *Polyhedron*, 1993, **12**, 1083.
21 N. L. Hill and H. Hope, *Inorg. Chem.*, 1974, **13**, 2079.
22 K. Henrick, P. A. Tasker and L. F. Lindoy, *Prog. Inorg. Chem.*, 1985, **33**, 1.
23 A. W. Addison, B. Watts and M. Wicholas, *Inorg. Chem.*, 1984, **23**, 813.
24 G. Reid, Ph.D. Thesis, University of Edinburgh, 1989; G. Reid and M. Schröder, unpublished work.
25 A. J. Blake, M. A. Halcrow and M. Schröder, *Acta Crystallogr., Sect. C*, 1992, **48**, 1844.
26 J. Cosier and A. M. Glazer, *J. Appl. Crystallogr.*, 1986, **19**, 105.
27 G. M. Sheldrick, SHELX 76, program for crystal structure refinement, University of Cambridge, 1976.
28 D. T. Cromer and J. B. Mann, *Acta Crystallogr., Sect. A*, 1968, **24**, 321.
29 G. M. Sheldrick, SHELXTL/PC version 4.3, University of Göttingen, Siemens Analytical X-Ray Instrumentation, Madison, WI, 1992.
30 R. O. Gould and P. Taylor, CALC, program for molecular geometry calculations, University of Edinburgh, 1985.
31 P. T. Beurskens, W. P. Bosman, H. M. Doesbury, Th.E.M. van den Hark, P. A. J. Prick, J. H. Noordik, G. Beurskens, R. O. Gould and V. Pathasarathia, DIRDIF, Applications of Direct Methods to Difference Structure Factors, University of Nijmegen, 1983.
32 N. Walker and D. Stuart, DIFABS, program for empirical absorption correction, *Acta Crystallogr., Sect. A*, 1983, **39**, 158.
33 G. M. Sheldrick, SHELXS 86, program for crystal structure solution, *Acta Crystallogr., Sect. A*, 1990, **46**, 467.

Received 23*rd December* 1993; *Paper* 3/07538I